bioresources.com

Comparative Study on the Effect of Bentonite or Feldspar Filled Low-Density Polyethylene/ Thermoplastic Sago Starch/Kenaf Core Fiber Composites

Norshahida Sarifuddin [a] and Hanafi Ismail [a,b]*

The present work evaluated the potential of the addition of bentonite and feldspar as fillers on the mechanical and physical properties of low-density polyethylene (LDPE)/thermoplastic sago starch (TPSS)/kenaf core fiber (KCF) composites. For this purpose, 3 to15 phr of fillers were incorporated into LDPE/TPSS/KCF composites that were fabricated via a melt-mixing molding system. Results showed that the tensile strength and modulus were improved significantly with the addition of bentonite in comparison with feldspar. Thermal studies confirmed the improvement in thermal stability of composites filled with bentonite as well as feldspar. An increased percentage of water absorption was also observed in these composites compared with the control (LDPE/TPSS/KCF composites) system.

INTRODUCTION

A major factor motivating the effort to develop new types of degradable materials is the never-ending waste disposal crisis caused by the high consumption of plastic materials. Plastics are inherently inert to microorganisms and chemicals in the environment. Thus, the disposal of a high volume of plastic, which takes a long time to decompose, poses a huge environmental problem. The rising concern about plastic waste disposal and the need for more versatile polymer-based material has led to increasing interest in blending synthetic polymers with degradable materials. Modified plastics derived from blends with agricultural feedstock such as starch have proved to be promising biopolymers to meet requirements and guarantee at least partial degradation (He *et al.* 2012). However, it has been found that the addition of thermoplastic starch as a minor ingredient in the synthetic thermoplastic matrix causes a reduction of the mechanical properties due to the immiscibility caused by the contrast between the hydrophilic and hydrophobic properties of the two constituents (Prachayawarakorn *et al.* 2010). Another interesting approach to improve mechanical properties and impart degradation is to use natural fibers to reinforce synthetic polymer/biopolymer blends. In light of recent global interest, kenaf is attracting special attention due to its good mechanical properties (Avella *et al.* 2008).

bioresources.com

Because there is great demand for new types of composite materials that can compensate for the drawbacks as well as add advantages to conventional composite materials, much attention has been paid to the development of composites in which two or more reinforcements are utilized in a matrix to obtain diverse properties in the composites (Muhammad Safwan *et al.* 2013). In view of the fact that organic and inorganic fillers possess their own advantages, utilization of fillers or blends or both in thermoplastics should offer synergistic effects (Ismail *et al.* 2010). Organic/inorganic material-filled composites have received significant attention from both academic and industrial groups. Organic fillers have the basic characteristics of low density, biodegradability, and sustainable productivity, and inorganic fillers have attracted great attention because of their cost efficiency and abundance. Recently, various thermoplastic composites prepared by the addition of fillers such as montmorillonite, mica, calcium carbonate, and carbon nanotubes have exhibited remarkable improvements in mechanical and thermal properties, dimensional stability, gas permeability, physicochemical behaviors, and biodegradability compared with neat thermoplastics (Nakamura *et al.* 2012). Through the incorporation of two types of fillers, the composites can become a prospective new class of materials (Nakamura *et al.* 2012). To date, studies have established that the addition of inorganic fillers to the natural fiber and polymer matrices can improve the mechanical and thermal properties of these composites. Some studies have reported on palm kernel shell/polypropylene filled with nanosilica (Muhammad Safwan *et al.* 2013), cellulose fiber–reinforced vinyl ester composites filled with halloysite nanotubes (Alhuthali and Low 2013), and poly(lactic acid)/newspaper fibers/talc hybrid composites (Huda *et al.* 2007).

Malaysia has long been known for having diverse types of mineral resources, such as barite, bauxite, clays, coal, copper, gold, iron ore, and silica. These minerals can be value-added in terms of properties through various processing techniques that enhance the application of these minerals (Suhaida *et al.* 2011). Thus, the current work aims to make use of the available inorganic fillers in diverse inventions. In general, the fundamental characteristics of fillers, such as shape, size, and surface nature, have great effects on the properties of composites. For that reason, bentonite and feldspar have been chosen for this study. Bentonite is a type of soft rock clay dominated by smectite group minerals with a small amount of biotite, quartz, and feldspar (Ismail and Mathialagan 2012). Feldspar is a group of rock-forming tectosilicate minerals. Bentonite exists in irregular shapes, whereas feldspar has a cubic shape. Both bentonite and feldspar can have a high adsorption capacity for polymers and are capable of exchanging ions on silicate layers with reactive hydroxyl (-OH) groups on the surface (Ismail and Mathialagan 2012; Ansari and Ismail 2009a).

Accordingly, it may be interesting to investigate the effect of shape, size, and the surface nature of inorganic fillers on the mechanical and physical properties of low-density polyethylene (LDPE)/thermoplastic sago starch (TPSS)/kenaf core fiber (KCF) composites. The hybridization of bentonite (Bt) and feldspar (Fs) with kenaf fibers in a LDPE/TPSS blend has not been reported. Incorporation of inorganic fillers was expected to enhance the mechanical and thermal properties of the polymer composites and decrease the volume of water intake.

EXPERIMENTAL

Materials

Sago starch (13% moisture) was obtained from the Land Custody Development Authority (LCDA), Sarawak, Malaysia. It had an average particle size of 20 µm and decomposition temperature of 230 °C. Glycerol (plasticizer) was an analytical grade reagent, purchased from Merck Chemicals (Malaysia) and used as received. Low-density polyethylene (LDF 260GG) with a melt flow index of 5 g/10 min was obtained from Titan (M) (Malaysia). Kenaf fibers (core) with an average length of 5 mm were supplied by National Kenaf and Tobacco Board (LKTN), Pasir Puteh, Kelantan, Malaysia. The fibers were subjected to a grinding process that yields particles approximately 70 to 250 µm in diameter. KCFs were then dried for 3 h at 70 °C in a vacuum before being used in subsequent composite fabrication. Bentonite was supplied by Ipoh Ceramics, Perak, Malaysia. The average particle size of the bentonite and the specific area are 23.1µm and 0.42 m^2/g, respectively (Othman *et al.* 2006). The chemical properties of bentonite are shown in Table 1. Feldspar (grade KM 325) was obtained from Commercial Minerals, Perak, Malaysia. The average particle size of the filler and the specific area are 13.6 µm and 0.73 m^2/g, respectively (Ansari *et al.* 2009). The chemical properties of feldspar are given in Table 2.

Table 1. Chemical Properties of Bentonite*

Chemical Composition (%)	Amount (%) (w/w)
SiO_2	67.0
Al_2O_3	15.0
Fe_2O_3	2.3
MgO	2.2
Na_2O	1.8
CaO	0.66
K_2O	0.55
TiO2	0.32
P_2O_5	0.02
MnO	0.04
NiO	0.02
ZnO	0.01

* (Othman *et al.* 2006)

Table 2. Chemical Properties of Feldspar *

Chemical Composition (%)	Amount (%) (w/w)
SiO_2	67.0
Al_2O_3	19.0
CaO	0.11
Na_2O	2.3
P_2O_5	0.18
SO_3	0.028
K_2O	11.0
Fe_2O_3	0.12
NiO	0.025
Rb_2O	0.28

* (Ansari *et al.* 2009)

Methods

Sample preparation

Sago starch powder was vacuum-dried by heating at 80 °C for 24 h before blending and processing. The dried sago starch was then pre-mixed with glycerol using a high-speed mixer. The weight ratio of sago starch to glycerol was maintained at 65:35 (wt%). The blend was stored overnight to allow the diffusion of glycerol into starch granules, which would help the melt-mixing process. The bentonite and feldspar in powder form as filler were dried at 105 °C in a convection oven for 24 h to expel moisture prior to use. Based on our previous work, the LDPE/TPSS ratio was fixed at 90:10, and the KCFs were constantly loaded at 10 phr. For this work, inorganic filler loading varied from 3 phr to 15 phr, as shown in Table 3. Mixing was carried out at 150 °C with a rotor speed of 50 rpm for a period of 20 min using an internal mixer Polydrive Thermo Haake R600. The processed samples were then compression-molded in an electrically heated hydraulic press (Kao Tieh Go Tech Compression Machine) at 150 °C into a 1-mm-thick sheet. Table 3 shows the formulation of the composites.

Table 3. Composite Formulation

LDPE (wt %)	TPSS (wt %)	KCF (phr)	Bentonite/Feldspar (phr)
90	10	10	0
90	10	10	3
90	10	10	6
90	10	10	9
90	10	10	12
90	10	10	15

Measurement of tensile properties

Tensile tests were carried out with a Universal Testing Machine (Instron 3366) according to ASTM D638. Dumbbell specimens of 1 mm thickness were cut from compression molded sheets with a Wallace die cutter. Tensile loading and displacement are measured directly by a load cell with capacity of 10 kN, gauge length of 50 mm and at strain rate of 10^{-2} s^{-1}.

A crosshead speed of 5 mm/min was used, and the test was performed at a temperature of 25 ± 3 °C and a relative humidity of $60 \pm 5\%$. Five replicate specimens were used to obtain average values for tensile strength, elongation at break, and Young's modulus.

Fourier Transform Infrared (FTIR) spectroscopy analysis

The changes in functional groups and chemical characteristics of LDPE/TPSS/KCF composites, bentonite-filled composites, and feldspar-filled composites were obtained by Fourier Transform Infrared Spectroscopy (FTIR, Perkin Elmer System 2000). The flat and smooth composite sheets (5 mm x 5 mm x 1mm) were simply placed on a Miracle ATR accessory (miracle base optic assembly) and the spectra were recorded in reflection, respectively. The FTIR spectra were recorded in a spectral range of 4000 to 600 cm^{-1} using 32 scans per sample with a resolution of 4 cm^{-1}.

Thermogravimetric analysis (TGA)

LDPE/TPSS/KCF composites, bentonite-filled composites and feldspar-filled composites samples were cut into small pieces (5 to 10 mg), which were then tested using thermogravimetric instruments (Perkin Elmer, Pyris Diamond TG/DTA) in a nitrogen atmosphere within a temperature range from room temperature to 550 °C at a heating rate of 15 °C/min. The thermal degradation temperature was reported as the onset degradation temperature, the point where the weight loss started to occur.

Morphology evaluation

Scanning electron micrographs of tensile fracture surfaces of LDPE/TPSS/KCF composites, bentonite-filled composites, and feldspar-filled composites samples were obtained using a scanning electron microscope (SEM, ZEISS Supra 35 VP). The samples were sputter-coated with a thin layer of carbon to avoid electrostatic charging during the examination. The image results were analyzed to investigate the distribution of natural fibers and inorganic fillers in the polymer matrix and their interactions.

Water absorption

Water uptake measurements were carried out per ASTM D570. Newly prepared samples were first dried in an oven at 70 °C for 24 h until a constant weight was attained and then dipped in distilled water at ambient temperature. After immersion for a specific interval, the samples were then removed from the water, gently dried by wiping with a clean cloth, and immediately weighed to the nearest 0.001 g. The percentage of water absorption was calculated as follows,

$$WA\ (\%) = [(M_1 - M_0)/M_0] \times 100 \tag{1}$$

where M_0 and M_1 are the dried weight and final weight of the sample, respectively.

RESULTS AND DISCUSSION

Processing Characteristics

The evaluation of the processing characteristic (mixing torque) becomes essential when internal mixing is employed to blend polymer composites. For this study the processing torques as a function of time were recorded and plotted to obtain the melt processing characteristics of LDPE/TPSS/KCF composites and their hybrid composites (filled with bentonite and/or feldspar). For comparison purposes, the bentonite and feldspar loading were fixed at 12 phr. The plotted curves are shown in Fig. 1. Nearly all composites showed a similar pattern of processing torque versus time curves.

The initial peak torques at approximately the first minute depicted the addition of solid material (LDPE) into the mixing chamber as well as the initiation of the rotor. Prior to melting, the addition of LDPE granules raised the torques due to the high shear force needed to rotate the rotor. Generally, the loading peak is highly dependent on the amount of LDPE injected into the mixing chamber. For this work, the amount of LDPE was fixed at 90 wt%. Thus, no significant difference in torque values within the first minute was observed with the addition of bentonite and feldspar fillers.
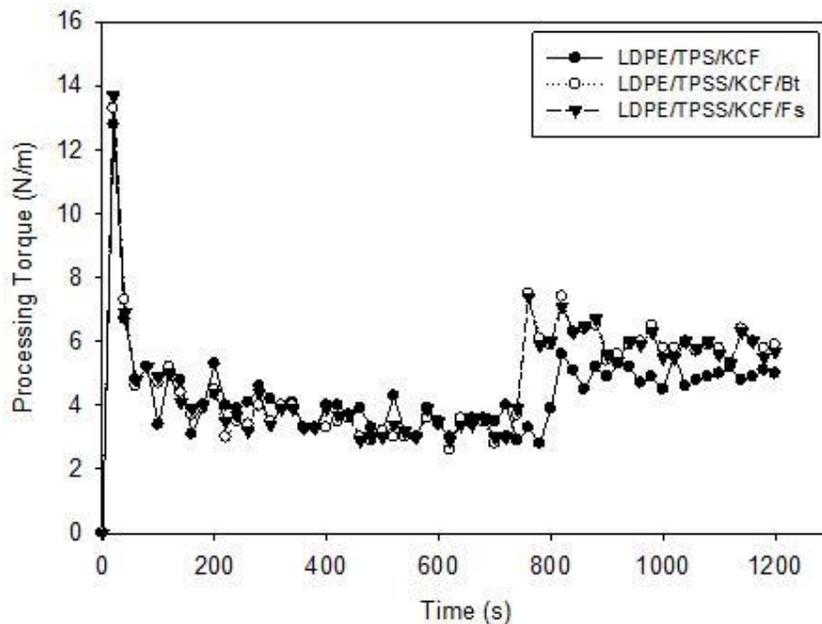
Fig. 1. Processing torques of LDPE/TPSS/KCF composites, bentonite-filled composites, and feldspar-filled composites

The viscosity of LDPE dropped down under shear and temperature, which then decreased the torque gradually, indicating the melting of LDPE (Othman *et al.* 2006). At 3 min, a small amount of TPSS was injected into the chamber. However, no prominent peak was obtained, which was attributed to the stable melt viscosity due to the presence of glycerol, which plasticized the blend (Kahar *et al.* 2012).

A sudden increase in torque was once again observed as the KCF/bentonite and KCF/feldspar fillers were loaded into the molten LDPE/TPSS at 13 min. The melt viscosity increased in the presence of fibers and inorganic fillers, which reduced the polymer chain mobility in the blend and consequently raised the torque values (Cao *et al.* 2011). The idea is that the presence of fibers and inorganic fillers gave rise to high shear force, resulting in high melt viscosity and yielding high mixing torque. Once the dispersion was completed and the mixture homogenized, the torque began to decrease and stabilize (Ansari and Ismail 2009a).

Stabilization torque is a measure of the average torque value between 18 min and 20 min of mixing. The stabilization torque of LDPE/TPSS/KCF composites, bentonite-filled composites and feldspar-filled composites are illustrated in Fig. 2. The results clearly indicate that composites with the addition of inorganic fillers exhibit higher stabilization torques than the control composites. Such an increase in stabilization torque could be due to the fine filler particles that form a large network and cause tighter packing, which will then augment the viscosity of the matrix as well as the overall composite systems. From Fig. 2, it can be observed that bentonite-filled composites yielded the highest stabilization torque values. This observation implies that incorporation of bentonite into the composites leads to a greater restriction of matrix mobility than feldspar-filled composites. It appears that the melt viscosity of the matrix increased due to the increasing obstruction of flow caused by these irregular-shaped

particles. These occurrences also might be due to the strong matrix-filler interaction and larger filler agglomerates, which consequently require high shear force and result in high stabilization torque.

On the contrary, lower stabilization torque values of feldspar-filled composites reflect the weaker matrix-filler interaction. The cubic-shaped structure of feldspar introduced discontinuity to the matrix, whereby lower viscosity may indicate slippage between filler particles and the polymer matrix and therefore lead to lower stabilization torque values.
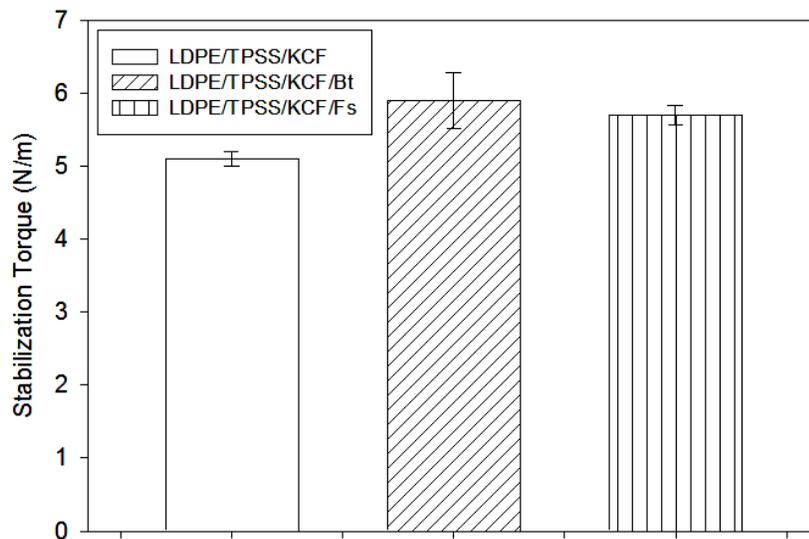
Fig. 2. Stabilization torques of LDPE/TPSS/KCF composites, bentonite-filled composites, and feldspar-filled composites

Tensile Properties

Figures 3, 4, and 5 demonstrate the effect of bentonite and feldspar loading on the tensile strength, elongation at break, and Young's modulus properties of LDPE/TPSS/KCF composites, respectively. Tensile properties of these composites are a function of how well the filler and polymer interact with each other. It was found that the tensile strength increased gradually with the addition of bentonite up to 12 phr (Fig. 3). However, the tensile strength declined as the loading of bentonite in the composite system further increased to 15 phr. Generally, the strength properties of the composite were strongly related to the interfacial interaction between the fillers and matrices. The tolerable specific surface area and particle size resulted in better dispersion of bentonite, which can easily penetrate between matrices and fibers (Ismail and Mathialagan 2012). The reinforcing mechanism was improved due to the synergistic effects that result from the different size, shape, and structure of hybrid fillers (Ismail and Mathialagan 2012). When sufficient contact area is provided to react with the polymer matrix, the wetting and adhesion of polymer to filler is also enhanced, which consequently allows better stress transfer (Suhaida *et al.* 2011). This occurrence is further explained in the morphological study. However, the agglomeration of fillers can be a possible explanation

for the reduction of tensile strength at higher filler loading. These fillers acted as stress concentrators, whereby applied stress was unable to be transferred from matrix to filler and larger agglomerates tended to initiate voids, which resulted in the failure of the composites.

Referring to Fig. 3, it can be deduced that the tensile strength was diminished as the loading of feldspar was increased from 3 to 15 phr. The incorporation of feldspar into the composite reduced the ability of the matrix to transfer applied stress, especially in the case of this filler with the cube shape. A similar finding was also observed by other researchers (Ansari and Ismail 2009b). Basically, it is believed that smaller particle size fillers such as feldspar provide more contact area with the polymer matrix due to their higher surface area in comparison with bentonite fillers. However, an adverse effect on strength was observed. Smaller particles seemed to cause agglomeration more than larger particles did (Gwon *et al.* 2011). In addition, it has been reported that the cubic-shaped structure of feldspar cannot disperse well in the matrix, sometimes forming clusters, which leads to higher cavity formation in the composites and reduces the interfacial interaction between polymer matrices and fillers (Gwon *et al.* 2011). When comparing the effect of fillers, it can be concluded that the bentonite gave rise to higher tensile strength than the feldspar.
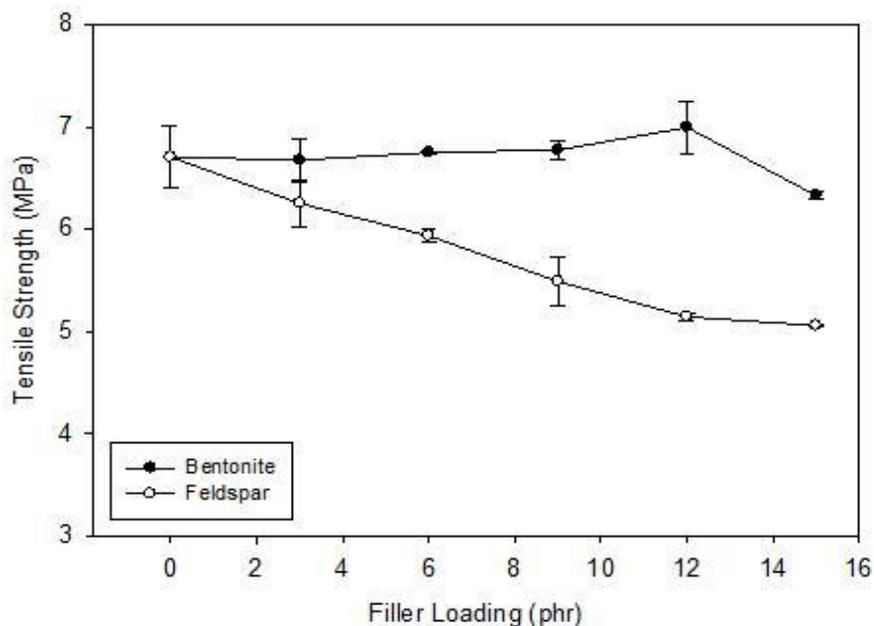

Fig. 3. Tensile strength of bentonite- and feldspar-filled composites at different filler loadings

On the other hand, Fig. 4 shows that the elongation at break decreased drastically with the addition of fillers. This phenomenon is common for polymeric materials strengthened with inorganic fillers. Inorganic reinforcing fillers are stiffer than the matrices and deform less, causing overall reduction in the matrix strain (Othman *et al.* 2006). The rate of change in elongation at break varied with the percentage of filler loading and was higher with smaller (feldspar) particles as compared with larger (bentonite) particles (Saleh and Mustafa 2011). The interstitial volume must have been

occupied by smaller particles, and insufficient matrices were therefore available to contribute to the percentage of elongation at break (Saleh and Mustafa 2011).
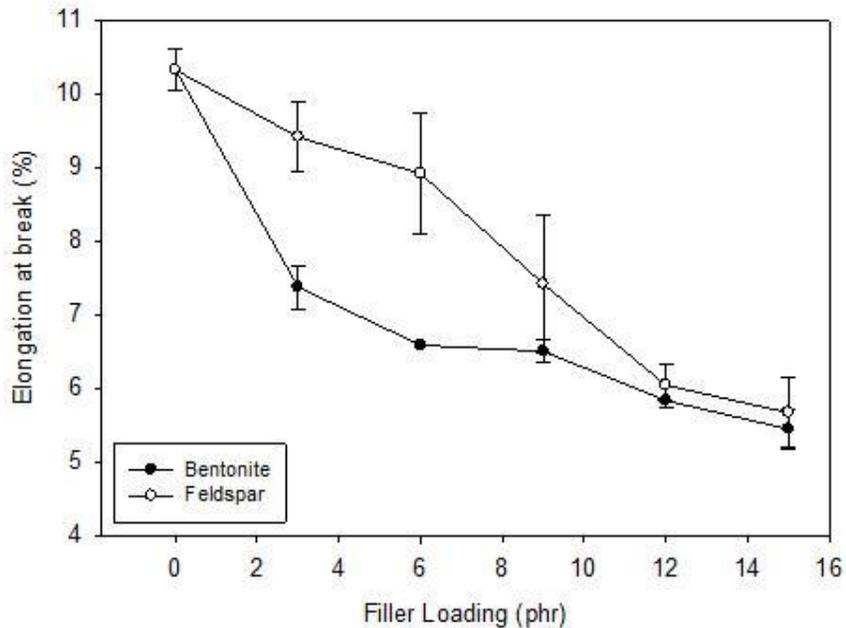

Fig. 4. Elongation at break of bentonite- and feldspar-filled composites at different filler loadings

From Fig. 5, it can be observed that increased filler content increased the Young's modulus of both composite systems. The presence of bentonite and feldspar produced a more rigid interface in the matrix, which then increased the stiffness of the composites (Ismail and Shaari 2010).
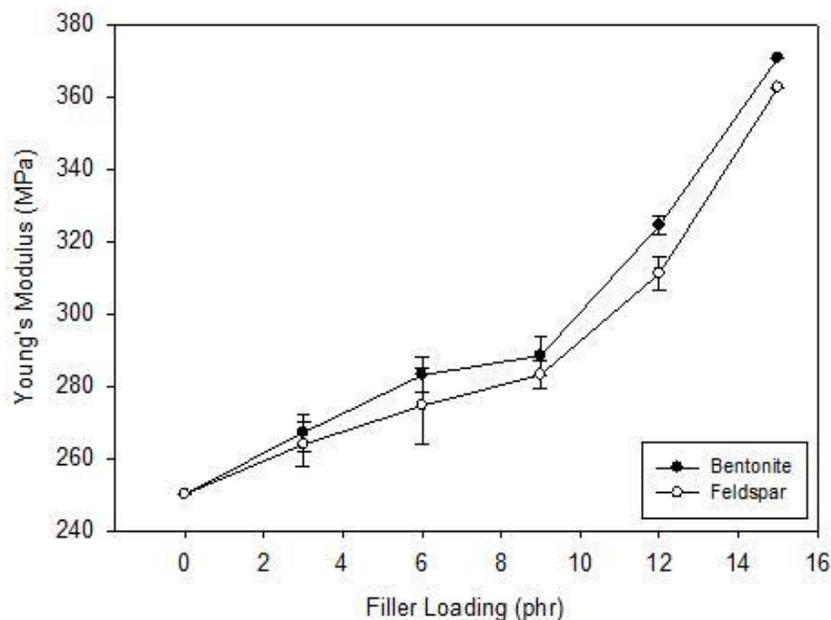
Fig. 5. Young's modulus of bentonite- and feldspar-filled composites at different filler loadings

The size and shape of both inorganic fillers in comparison with kenaf fibers gave heterogeneous mechanical properties to the composites. Theoretically, the modulus of the composite will be higher when small particles such as feldspar are used. Perhaps smaller particles occupied the interstitial volume, and hence the surface area for deformation was higher than with larger particle sizes (Saleh and Mustafa 2011). However, in this case, bentonite has sufficient surface area to complement an interfacial interaction with a polymer matrix. Hence, bentonite is expected to hinder the mobility of the surrounding chains in the polymer matrix and increase the matrix stiffness (Alhuthali and Low 2013).

Fourier Transform Infrared (FTIR) Spectroscopy Analysis

Figure 6 shows the FTIR spectra of LDPE/TPSS/KCF composites, bentonite-filled composites and feldspar-filled composites. FTIR analysis reveals possible structural information and examines the bond interaction between all components in the composite system. The bentonite and feldspar loading was fixed at 12 phr so that a comparison could be made to study the effects of these filler addition on the composites.

As seen in Fig. 6, the spectra of the control composites revealed characteristic peaks at 3360 cm^{-1}, 2915 cm^{-1}, 2848 cm^{-1}, 1646 cm^{-1}, 1463 cm^{-1}, and 718 cm^{-1} which was attributed to stretching vibrations of –OH, C-H stretching, C=O stretching, -CH$_3$ bending, and –CH$_2$ vibration, respectively.
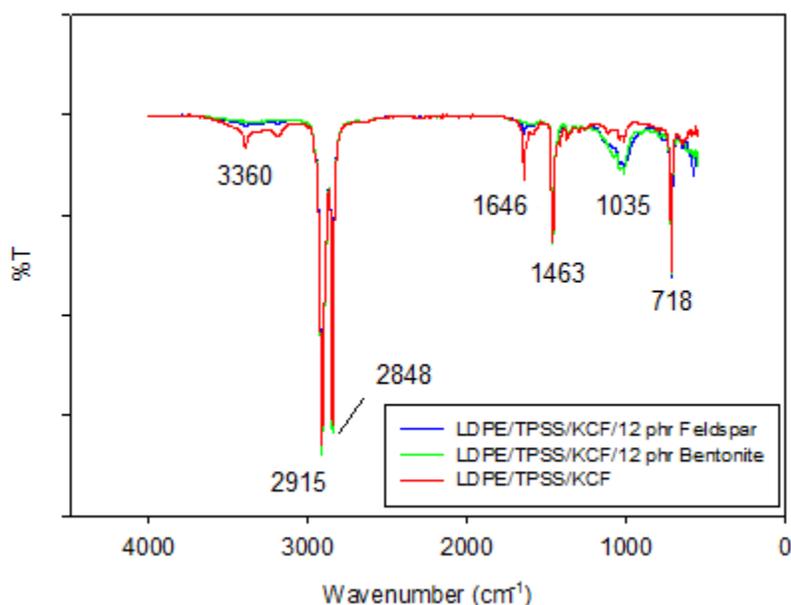

Fig. 6. FTIR spectra of LDPE/TPSS/KCF, LDPE/TPSS/KCF/12 phr bentonite and LDPE/TPSS/KCF/12 phr feldspar composites

Referring to spectra of bentonite- and feldspar-filled composites in comparison to the control composites, it was found that all spectra were matched closely with one another. However, the presence of bentonite and feldspar fillers caused slight changes in band positions and intensities. It was observed that the intensity of the peak corresponding to -OH stretching was decreased and slightly shifted. The decrease in intensity and shifting of the band suggested the participation of hydroxyl group of

bioresources.com

inorganic fillers in reaction with TPSS and KCF. Moreover, the intensities of peak 1035 cm^{-1}, which were assigned for the Si-O-Si stretching band (Alhuthali and Low 2013), were more pronounced compared to the control composites corresponding to the presence of bentonite and feldspar fillers in the composites. The appearances of all characteristic peaks were correlated to the distribution and dispersion of inorganic fillers in the composites. Slight changes in peak intensities and band positions exhibited a distinct interaction between chains of polymers and other components.

Thermogravimetric Analysis (TGA)

Thermogravimetric analysis was carried out to evaluate the thermal stability and degradation temperature of the control LDPE/TPSS/KCF composites, bentonite-filled composites, and feldspar-filled composites. Figure 7 shows the TGA profiles of raw bentonite and feldspar fillers, LDPE/TPSS/KCF composites, LDPE/TPSS/KCF/Bt (12 phr) composites, and LDPE/TPSS/KCF/Fs (12 phr) composites. The data for initial thermal degradation, maximum weight loss, and end degradation temperature are summarized in Table 4.

As can be seen in Fig. 7, the initial weight loss of raw bentonite was found at 84.2 °C, and the temperature at maximum degradation was 104.2 °C, with a total weight loss of 15.9%, whereas in the case of raw feldspar, the degradation occurred at 139.1 °C, with a maximum weight loss of 0.70%.

For LDPE/TPSS/KCF composites, the TGA profile demonstrated a small weight loss below 200 °C caused by the volatilization of adsorbed water. Mass loss at approximately 300 to 370 °C was mainly due to thermal decomposition of starch and volatilization of glycerol as well as cellulosic substances. The thermal degradation above 400 °C was associated with the greatest weight loss and was due to the thermal degradation of the LDPE backbone (Belhassen *et al.* 2009). For these composites, maximum weight loss was obtained at 97.5%. These occurrences were attributed to the higher thermal stability of fibers and phase compatibility between TPSS and KCF, which consequently reduced heat flow to the composite and inhibited the degradation process.

The incorporation of bentonite in LDPE/TPSS/KCF composites decreased the initial degradation temperature to 294.2 °C and the end degradation temperature to 494.1 °C, in contrast to the control composites. Accordingly, the maximum weight loss was reduced to 86.4% with 12 phr bentonite loading. Figure 7 demonstrates an enhancement in the thermal stability of bentonite-filled composites compared with samples without bentonite. It was assumed that the improvement in thermal stability was the result of reduction in weight loss (Wang *et al.* 2005). Because bentonite has no weight loss at low temperature, the residue mass increased. This factor can account for the improved thermal stability. In addition, the presence of metal oxides in bentonite such as silica, aluminum, iron, and magnesium also can contribute to this improvement (Othman *et al.* 2006).

Referring to the TGA profile in Fig. 7, composites with 12 phr feldspar loading exhibited better thermal stability than the control composites and bentonite-filled composites with higher residue mass, as the maximum weight loss was found at 85.1%. The remarkable reduction in mass loss of this composite resulted from the fact that during combustion, the silicate layers with high aspect ratios were able to migrate toward the material surface, followed by a char barrier layer formation, which could sustain high temperatures and hinder heat and mass transfer efficiently (Hemati and Garmabi 2011).

This enhancement in thermal properties supposedly contributed to the flame retardation potential (Alamri *et al.* 2012).

From the amounts of residue, it can be concluded that the presence of inorganic filler slightly decreased the rate of sample degradation compared to the control composites. But the maximum decomposition temperature of the composites remained unchanged after the addition of bentonite as well as feldspar.

Table 4. Thermogravimetric Analysis of Hybrid Composites

Sample	Temperature at 5% Weight Loss ($T_{5\%}$) (°C)	Maximum Weight Loss (%)	Temperature at Maximum Weight Loss (T_{max}) (°C)
Bentonite (Bt)	84.2	15.9	104.2
Feldspar (Fs)	-	0.7	139.1
LDPE/TPSS/KCF	305	97.5	494
LDPE/TPSS/KCF/Bt	294.2	86.4	494.1
LDPE/TPSS/KCF/Fs	289.2	85.1	494.2
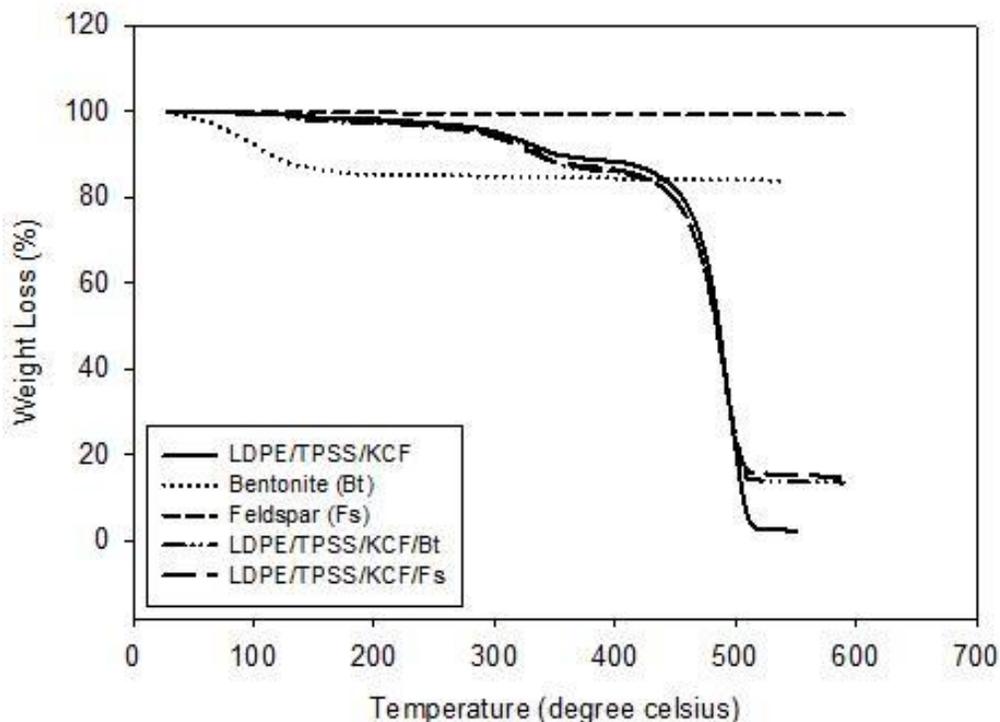
Fig. 7. TGA profiles of inorganic fillers and their composites

Water Absorption

To identify the durability of a composite, it is necessary to understand its water absorption behavior. The absorption behavior is found by the immersion of composites in

water at ambient temperature and the measurement of the rate of water diffusion into the composite. In the initial stage of the absorption process, kinetic absorption occurred rapidly, and the absorption rate gradually slowed down until reaching equilibrium. Figure 8 illustrates the percentage of water absorption of the control LDPE/TPSS/KCF composites, bentonite-filled composites, and feldspar-filled composites. The filler loading was fixed at 12 phr so that a comparison could be performed to evaluate the effect of various fillers on the composites.
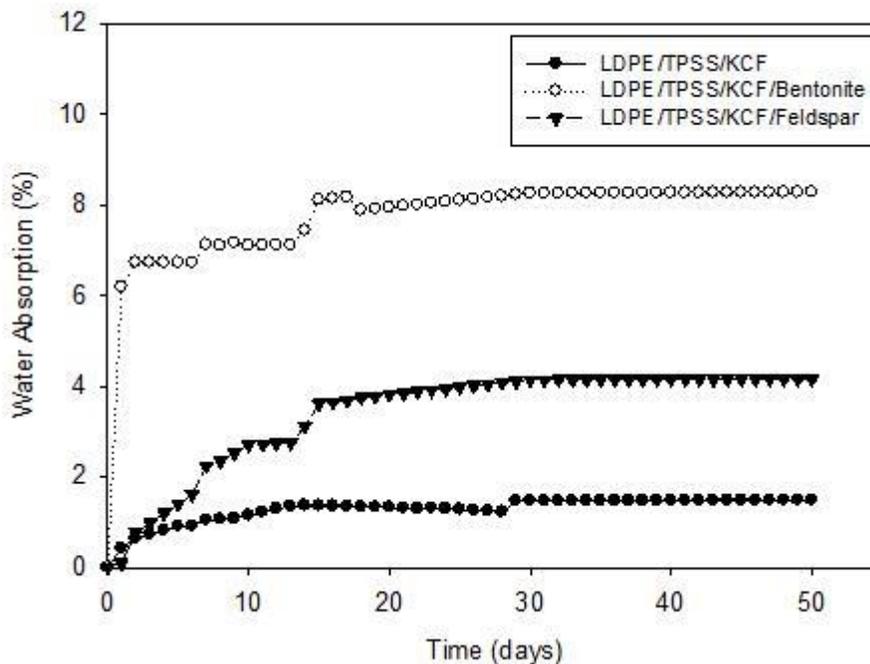
Fig. 8. Water absorption behavior of LDPE/TPSS/KCF, LDPE/TPSS/KCF/bentonite, and LDPE/TPSS/KCF/feldspar composites

As for the control LDPE/TPSS/KCF composites, the existence of LDPE in the composite could theoretically dramatically restrain water absorption and reduce water sensitivity due to the hydrophobic characteristic of non-polar LDPE. However, it is interesting to note that the observed rise in water absorption capacity was highly dependent on KCF and TPSS content. The rise in water uptake was attributed to the hydrophilic nature of starch and fiber by virtue of the presence of abundant hydroxyl groups available for interaction with water molecules.

It was expected that bentonite and feldspar fillers would create denser composite networks, thus blocking water from entering the system as the path filled with filler. However, the incorporation of bentonite and feldspar in the composite system showed a significant increase in water uptake capacity over time. This was attributed to the hydrophilicity of the filler surface as well as an increase in the void fraction between fillers and matrics generated during processing. This phenomenon decreased the ability of the composite material to hold water during its service life (Saleh and Mustafa 2011). Accordingly, for the surface nature, bentonite showed a stronger hydrophilic nature than feldspar. Due to the exposure of many hydroxyl groups on the surface of bentonite, the

hydrophilicity of the filler surface was higher for bentonite than for feldspar. Therefore, the bentonite surface could attract a larger relative amount of water than the feldspar (Gwon *et al.* 2011). In addition, it is worth noting that higher filler content resulted in more voids being entrapped, leading to higher water accumulation at the interface between fiber and matrix. The low degree of adhesion between hydrophobic LDPE and hydrophilic TPSS, and the fillers' yield in the cracks and the voids between them, allowed for the easy penetration of moisture and the storage of water in the voids. Thus, the percentage of water uptake rose significantly.

## Morphological Study of Tensile Fracture Surfaces

The SEM micrographs of raw bentonite and feldspar as well as the tensile fractured surface of their composites are depicted in Fig. 9a–i. The morphology of raw bentonite is shown in Fig. 9a. Bentonite particles have irregular shapes with rough surfaces consisting of pores and voids (Ismail and Mathialagan 2012). It is believed that the obtained tensile strength is beneficially affected by the presence of pores and voids, which increase the specific area of bentonite for better adhesion, resulting in penetration of the matrix into the bentonite particles (Ismail and Mathialagan 2012). Figure 9b shows the SEM micrographs of raw feldspar fillers, which reveals that the majority of feldspar exists in a mass cube shape. The presence of many feldspar particles clustered together has been observed.

Figure 9c meanwhile illustrates the tensile fracture surface of LDPE/TPSS/KCF composites. It can be seen that the kenaf fibers were well dispersed and embedded in the matrix. It seems that the fiber surface was wetted by the polymer matrix. Simultaneously, there were microvoid or vacant spots in between the fibers and matrices. However, the composites filled with 6 phr bentonite displayed in Fig. 9d show that the bentonite particles were filling in the vacancies or microvoids, in contrast to the control composites. The bentonite particles can be perfectly distinguished within the matrices and fibers. However, with low loading of fillers in the composites, it is confirmed that there was an inhomogeneous distribution of bentonite, indicated by occasional micron-size aggregates scattered within the matrix. Increasing amounts of bentonite up to 12 phr yielded a composite with a rougher fracture surface and more matrix tearing, as shown in Fig. 9e. Although there were still many holes due to fiber pull-out, the rough surface area correlates with the higher tensile properties (Ismail and Mathialagan 2012; Gwon *et al.* 2011). The irregular shape of bentonite provides sufficient surface area to permit this filler to disperse well, fix in the polymer chain, and link the fiber and matrix, establishing a good interfacial interaction (Suhaida *et al.* 2011). On the other hand, SEM micrographs in Fig. 9f exhibit agglomeration of bentonite particles in the composite system that act as stress concentration points with a greater probability of composites initiating cracks (Ismail and Mathialagan 2012). Increased filler content led to large agglomerates and consequently resulted in the formation of small voids observed at the fracture surface. This is due to the detachment of bentonite agglomerates from the matrix, which indicates poor interfacial interaction between the matrix and filler.

The SEM morphology of hybrid composites filled with 6 phr feldspar (Fig. 9g) exhibits feldspar particles embedded within the matrices with less filler detachment and no filler agglomeration, which correlates with high tensile strength, whereas a large detachment of feldspar particles was seen when filler loading was increased up to 12 phr, as depicted in Fig. 9h. The cubical and elongated feldspar showed poor dispersion in the

matrix, as agglomeration can clearly be seen (Suhaida *et al.* 2011). In fact, the non-reinforcing nature of feldspar yields less interfacial interaction between components in composite systems, which subsequently leads to opening of voids. The situation became worse when more feldspar particles were incorporated into the composites. Figure 9i exhibits the fracture surface of 15 phr feldspar-filled composites. Feldspar agglomerates are visible, and their occurrence significantly reduced tensile strength. This is because agglomerations of feldspar act as stress concentrators and tend to initiate cracks. As a result, many voids and cavities were observed due to detachment of feldspar agglomerates from the matrix.
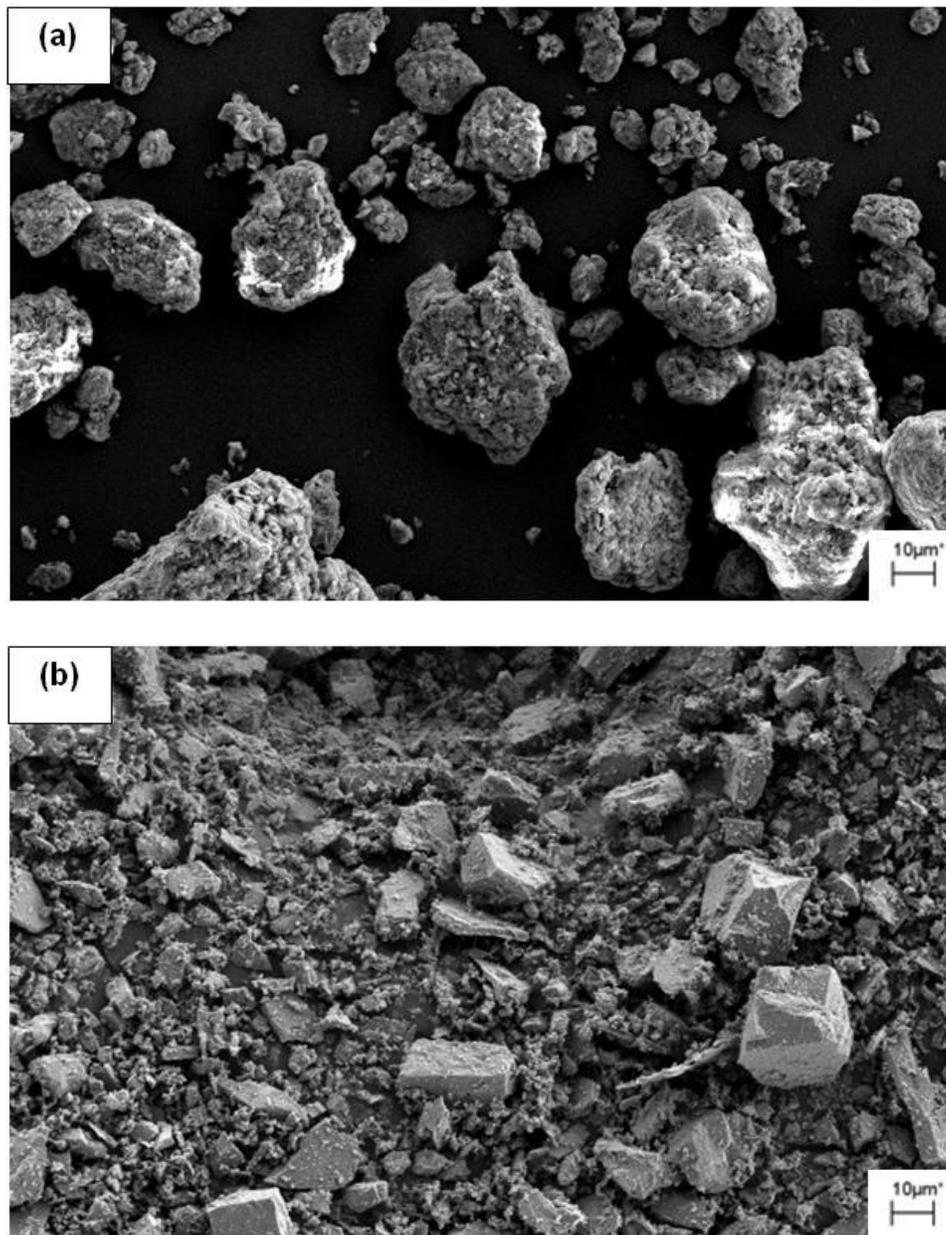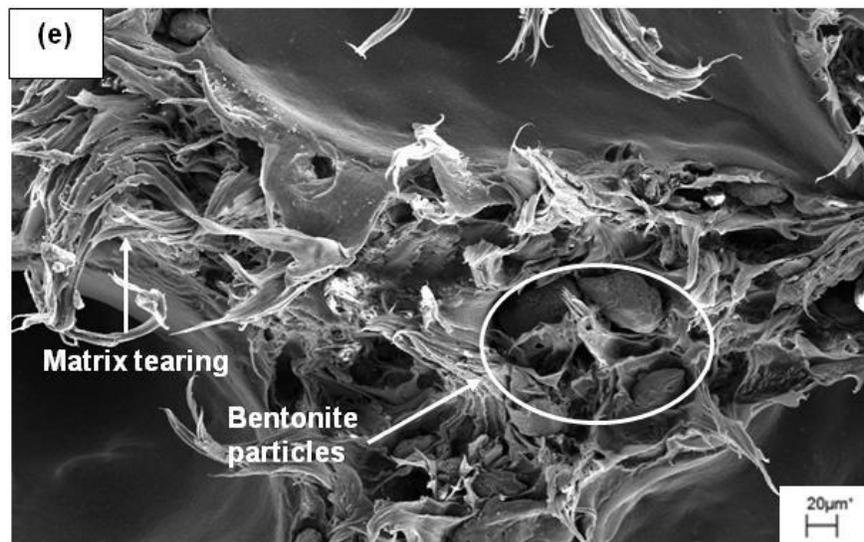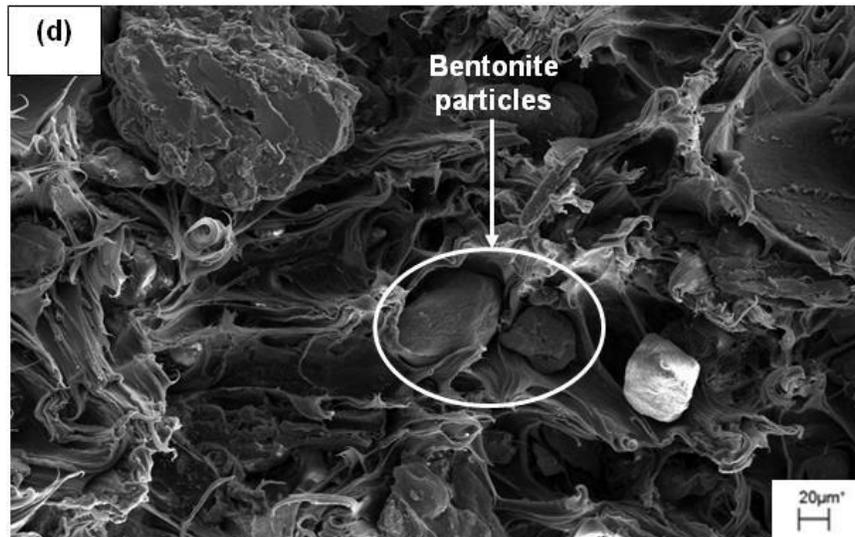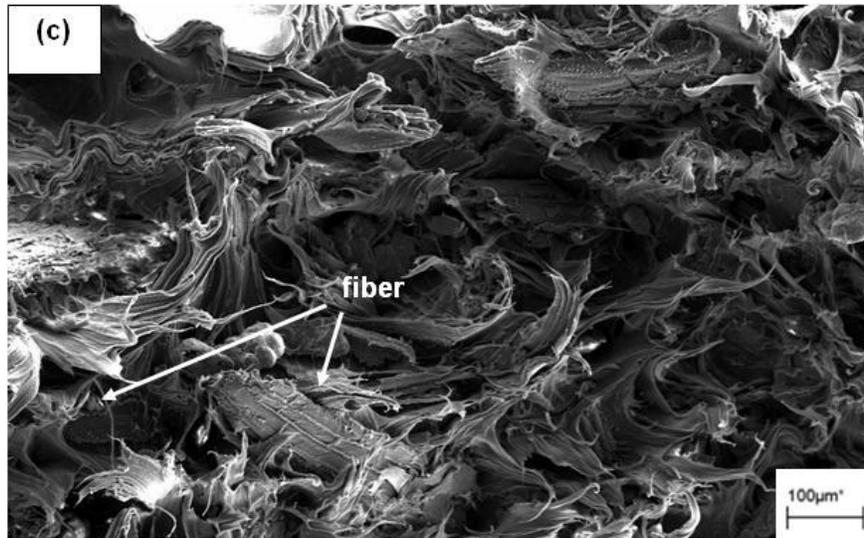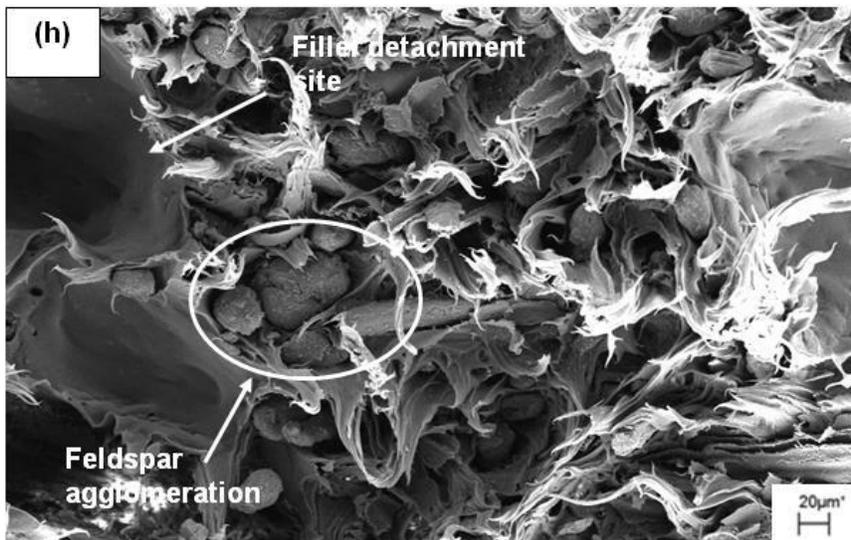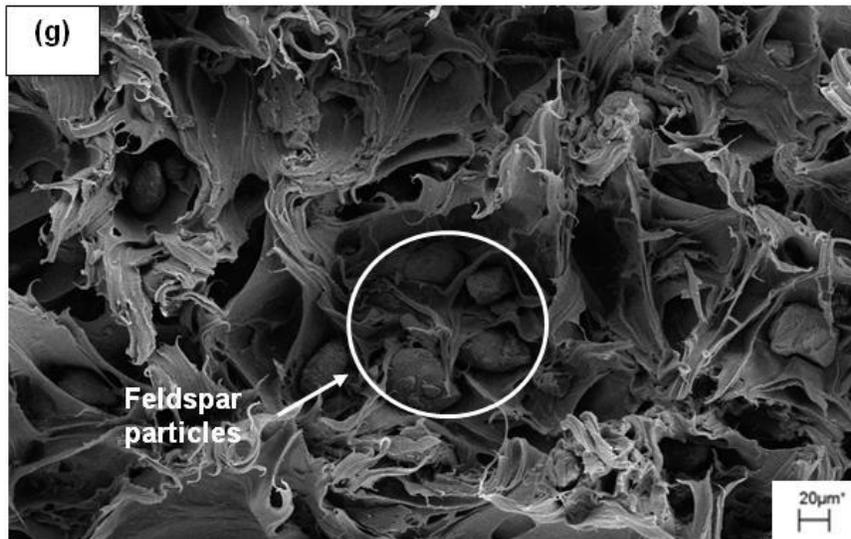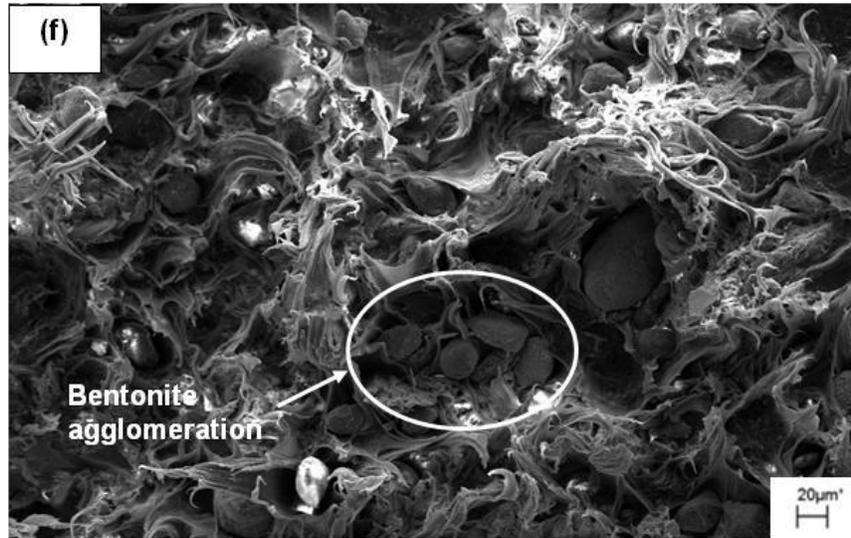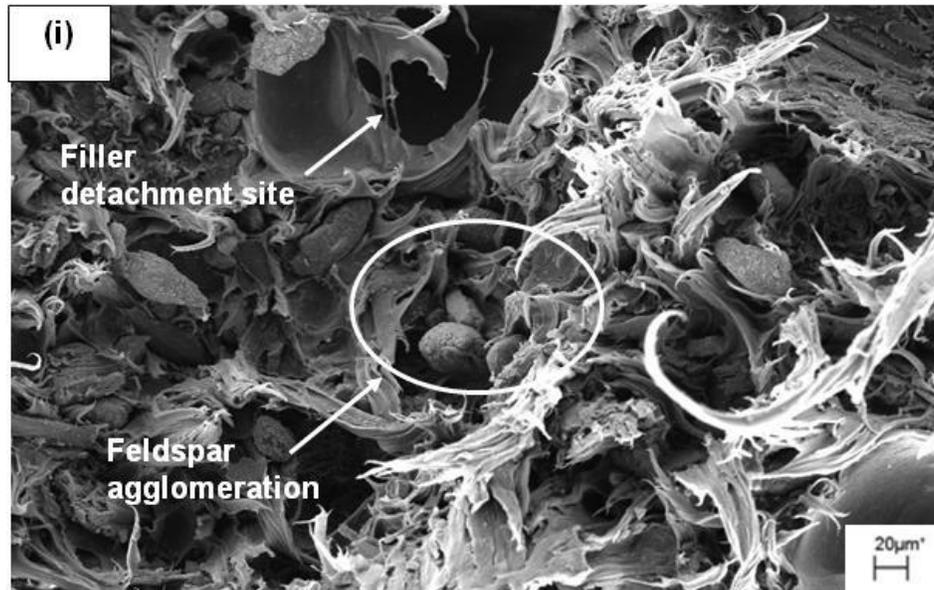
Fig. 9. SEM micrographs of (a) raw bentonite (500✕), (b) raw feldspar (500✕), (c) LDPE/TPSS/KCF (100✕), (d) LDPE/TPSS/KCF/6 phr bentonite (200✕), (e) LDPE/TPSS/KCF/12 phr bentonite (200✕),(f) LDPE/TPSS/KCF/15 phr bentonite (200✕), (g) LDPE/TPSS/KCF/6 phr feldspar (200✕),(h) LDPE/TPSS/KCF/12 phr feldspar (200✕) and (i) LDPE/TPSS/KCF/15 phr feldspar (200✕)

CONCLUSIONS

1. The effects of inorganic fillers (bentonite and feldspar) on the physical and mechanical properties of LDPE/TPSS/KCF composite systems were demonstrated. It was observed that the tensile strength and modulus of the blend could be effectively improved by the incorporation of bentonite in comparison with feldspar. As expected, elongation at break showed the reverse effect. FTIR analysis further showed that the reaction between all components took place through the occurrence of bonding between functional groups.

2. Thermal degradation temperatures and the thermal stability of LDPE/TPSS/KCF composites were also slightly improved by the addition of bentonite as well as of feldspar.

3. Concerning water absorption, increasing the amount of filler led to a rise in the water uptake capacity of the composites.

4. Morphological studies provided by SEM micrographs revealed that the size, shape, and surface nature of bentonite and feldspar greatly affected the interfacial interaction between fillers and matrices.

ACKNOWLEDGMENTS

REFERENCES CITED

Alamri, H., Low, I. M., and Alothman, Z. (2012). "Mechanical, thermal, and microstructural characteristics of cellulose fiber reinforced epoxy/organoclay nanocomposites," *Composite Part B* 43(7), 2762-2771.

Alhuthali, A. M., and Low, I. M. (2013). "Influence of halloysite nanotubes on physical and mechanical properties of cellulose fibers reinforced vinyl ester composites," *Journal of Reinforced Plastics & Composites* 32(4), 233-247.

Ansari, M. N. M., and Ismail, H. (2009a). "Effect of compatibilizers on mechanical properties of feldspar/polypropylene composites," *Polymer-Plastic Technology and Engineering* 48(12), 1295-1303.

Ansari, M. N. M., and Ismail, H. (2009b). "The effect of silane coupling agent on mechanical properties of feldspar filled polypropylene composites," *Journal of Reinforced Plastics and Composites* 28(24), 3049-3060.

Ansari, M. N. M., Ismail, H., and Zein, S. H. S. (2009). "Effect of multi-walled carbon nanotubes on mechanical properties of feldspar filled polypropylene composites," *Journal of Reinforced Plastics and Composites* 28(20), 2473-2485.

Avella, M., Bogoeva-Gaceva, G., Buzarovska, A., Errico, M. E., Gentile, G., and Grozdanov, A. (2008). "Poly(lactic acid)-based biocomposites reinforced with kenaf fibers," *J. Appl. Polym. Sci*. 108, 3542-3551.

Belhassen, R., Boufi, S., Vilaseca, F., Lopez, J .P., Mendez, J. A., Franco, E., Pelach, M. A., and Mutje, P. (2009). "Biocomposites based on alfa fibers and starch-based biopolymer," *Polym. Adv. Technol.*20(12), 1068-1075.

Cao, X. V., Ismail, H., Rashid, A. A., Takeichi, T., and Huu, T. V. (2011). "Mechanical properties and water absorption of kenaf powder filled recycled high density polyethylene/natural rubber biocomposites using mape as a compatibilizer," *BioResources* 6(3), 3260-3271.

Gwon, J. G., Lee, S. Y., Chun, S. J., Doh, G. H., and Kim, J. H. (2011). "Physical and mechanical properties of wood-plastic composites hybridized with inorganic fillers," *Journal of Composite Materials* 46(3), 301-309.

He, Y., Kong, W., Wang, W., Liu, T., Gong, Q., and Gao, J. (2012). "Modified natural halloysite/potato starch composite films," *Carbohydrate Polymers* 87, 2706-2711.

Hemati, F., and Garmabi, H. (2011). "Compatibilised LDPE/LLDPE/nanoclay nanocomposites: Structural, mechanical and thermal properties," *The Canadian Journal of Chemical Engineering* 89(1), 187-196.

Huda, M. S., Drzal, L. T., Mohanty, A. K., and Misra, M. (2007). "The effect of silane treated and untreated talc on the mechanical and physic-mechanical properties of poly (lactic acid)/newspaper fibers/talc hybrid composites," *Composites Part B* 38, 367-379.

Ismail, H., and Mathialagan, M. (2012). "Comparative study on the effect of partial replacement of silica or calcium carbonate by bentonite on the properties of EPDM composites," *Polymer Testing* 31(2), 199-208.

Ismail, H., and Shaari, S.M. (2010). "Curing characteristics, tensile properties and morphology of palm ash/halloysite nanotube/ethylene-propylene-diene monomer (EPDM) hybrid composites," *Polymer Testing* 29(7), 872-878.

Ismail, H., Norjulia, A. M., and Ahmad, Z. (2010). "Curing characteristic, mechanical and morphological properties of kenaf fibers/halloysite nanotubes hybrid-filled natural rubber compounds," *Polymer-Plastic Technology and Engineering* 49(9), 938-943.

Kahar, A. W. M., Ismail, H., and Othman, N. (2012). "Effects of polyethylene-grafted maleic anhydride as a compatibilizer on the morphology and tensile properties of (thermoplastic tapioca starch)/(high-density polyethylene)/(natural rubber) blends," *J. Vinyl and Additive Technol*. 18(1), 65-70.

Muhammad Safwan, M., Lin, O. H., and Md. Akil, H. (2013). "Preparation and characterization of palm kernel shell/polypropylene biocomposites and their hybrid composites with nanosilica," *BioResources* 8(2), 1539-1550.

Nakamura, R., Netravali, A. N., Morgan, A. B., Nyden, M .R., and Gilman, J. W. (2012). "Effect of halloysite nanotubes on mechanical properties and flammability of soy protein based green composites," *Fire and Materials* 37(1), 75-90.

Othman, N., Ismail, H., and Mariatti, M. (2006). "Effect of compatibilizers on mechanical and thermal properties of bentonite filled polypropylene composites," *Polymer Degradation and Stability* 91, 1761-1774.

Prachayawarakorn, J., Hommanee, L., Phosee, D., and Chairapaksatien, P. (2010). "Property improvement of thermoplastic mung bean starch using cotton fiber and low-density polyethylene," *Starch–Stärke* 62(8), 435-443.

Saleh, N. J., and Mustafa, S. M. (2011). "A study of some mechanical, thermal and physical properties of polymer blend with Iraqi kaolin filler," *Engineering and Technology Journal* 29(11), 2114-2132.

Suhaida, S. I., Ismail, H., and Palaniandy, S. (2011). "Study of the effect of different shapes of ultrafine silica as fillers in natural rubber compounds," *Polymer Testing* 30(2), 251-259.

Wang, S., Yu, J. G., and Yu, J. L. (2005). "The compatible thermoplastic starch/ polyethylene blends by one-step reactive extrusion," *Polym. Int.* 54(2), 279-285.